J Arid Land (2023) 15(11): 1340–1354
https://doi.org/10.1007/s40333-023-0032-5

Science Press Springer-Verlag

Contribution of groundwater to the formation of sand dunes in the Badain Jaran Desert, China

WANG Wang[1], CHEN Jiaqi[2*], CHEN Jiansheng[3], WANG Tao[4], ZHAN Lucheng[4], ZHANG Yitong[1], MA Xiaohui[5]

[1] College of Civil and Transportation Engineering, Hohai University, Nanjing 210098, China;
[2] School of Computer and Information, Hohai University, Nanjing 210098, China;
[3] Water Science Research Institute, Hohai University, Nanjing 211100, China;
[4] College of Water Conservancy and Hydropower Engineering, Hohai University, Nanjing 210098, China;
[5] Water Affairs Integrated Service Centre of Alagxa League, Inner Mongolia Autonomous Region, Alagxa League 750300, China

Abstract: The tallest sand dune worldwide is located in the Badain Jaran Desert (BJD), China, and has been standing for thousands of years. Previous studies have conducted limited physical exploration and excavation on the formation of sand dunes and have proposed three viewpoints, that is, bedrock control, wind dominance, and groundwater maintenance with no unified conclusion. Therefore, this study analyzed the underlying bedding structure of sand dunes in the BJD. Although the bedrock of sand dunes is uplifted and wind controls the shape of dunes, the main cause of dune formation is groundwater that maintains the deposition of calcareous sandstone and accumulation of aeolian sand. According to water transport model and vapor transports in the unsaturated zone of sand dunes, capillary water transport height is limited with film water constituting the main form of water in dunes. Chemical properties and temperature of groundwater showed that aquifers in different basins receive relatively independent recharge from deep sources in the crater. Result of dune formation mechanism is of considerable importance in understanding groundwater circulation and provides a new perspective on water management in arid desert areas.

Keywords: sand dune formation; groundwater; unsaturated zone; water content; desert water resource

Citation: WANG Wang, CHEN Jiaqi, CHEN Jiansheng, WANG Tao, ZHAN Lucheng, ZHANG Yitong, MA Xiaohui. 2023. Contribution of groundwater to the formation of sand dunes in the Badain Jaran Desert, China. Journal of Arid Land, 15(11): 1340–1354. https://doi.org/10.1007/s40333-023-0032-5

1 Introduction

Dunes are common landforms in arid and semi-arid areas on the Earth (Lancaster et al., 2002; Parteli and Herrmann, 2007; Lorenz and Radebaugh, 2009; Gunn et al., 2022). Their genesis and morphology are affected by many complex factors (Lancaster et al., 2002; Hesse, 2011; Ping et al., 2014; Meng et al., 2022) including climate, geographical position, surrounding sand sources, and hydrological conditions. Therefore, the characteristics and changes in the environment can be reflected. The tallest dune in the world is located in the Badain Jaran Desert (BJD) in northwestern Inner Mongolia Autonomous Region, China (Yan et al., 2001; Yang et al., 2010; Zhang et al., 2021). The BJD is the second largest desert in China, located in the middle of the westerly circulation and the tail of the East Asian summer monsoon (Hu and Yang, 2016). Many

*Corresponding author: CHEN Jiaqi (E-mail: jiaqichen@hhu.edu.cn)
Received 2023-06-28; revised 2023-10-12; accepted 2023-10-25

studies have been conducted on desert environments and geomorphic formations (Chen et al., 2004; Chen et al., 2006; Dong et al., 2009; Dong et al., 2013; Zhang et al., 2021). One of the core issues that needs to be solved is the long-term stability of tall dunes (Zhu, 2023). Based on particle size analysis of aeolian sand and rare earth elements, lacustrine deposits, and alluvial fans in the western and northwestern BJD, Gobi erosion is the main sand sources (Hu and Yang, 2016; Zhang et al., 2021). According to the occurrence of calcareous cement layers in sand dunes and the results from photoluminescence dating, researchers believed that since the early Pleistocene, sand dunes have gradually formed under dominant westerly wind (Yan et al., 2001). With the development of remote sensing technology, the prevailing westerly winds have been shown to affect the formation of sand dunes and result in a complex morphology (Dong et al., 2009; Yang et al., 2010). The dunes in the hinterland of the BJD, where mega-dunes are concentrated, are oriented mainly northeast and northern northeast, in line with the prevailing westerlies (Yang et al., 2011). However, mega-dunes here over 100 m high are not only from wind. Some researchers speculated that the underlying bedrock was the cause, but to date, this has not been confirmed because of the lack of deep drilling on the dunes and the limitations of physical detection methods (Bai et al., 2011; Dong et al., 2013; Qian and Liu, 2015).

At the foot of dunes, spring water is usually exposed with the total dissolved solids (TDS) less than 1 g/L despite severe surface salinization (Luo et al., 2016; Zhao et al., 2017). Since the end of the last century, it has been noticed that wet sand layers with high water content commonly exist below the surface of mega-dunes, which is in strong contrast to the local dry climate (Gu et al., 2004; Qian and Liu, 2015). The soil water content in the mega-dunes (with a height of 300–400 m) could reach 3% at a depth of 20 cm (Gu et al., 2004), which plays an important role in sand resistance to wind erosion. Therefore, groundwater is believed to maintain mega-dunes (Chen et al., 2004). Compared with other deserts in China, the BJD has a higher wind speed and coarser sand particle size (Zhao et al., 2011). Results of ^{14}C dating of rhizoconcretions, organic matter, and freshwater organisms have shown that sand dunes and lakes have coexisted in the desert for thousands of years and their positions are relatively fixed (Yang et al., 2010; Yang and Scuderi, 2010). The BJD is one of the biggest contributors to dust emissions in northern China (Wei et al., 2022), but the mega-dunes in the hinterland of the desert are still standing with over 100 permanent lakes (Yang, 2003). The close distribution of high dunes and inter-dune lakes and the correlation between lake area and sand dune height, have led researchers to discover that the two have similar formation mechanisms related to groundwater (Dong et al., 2013; Zhu, 2023). Moreover, the water table in the dunes is higher than the surrounding lake (Chen et al., 2004; Qian and Liu, 2015), indicating that groundwater may flow from the dunes to nearby lakes. Therefore, the formation and development of dunes requires further study, particularly the influence of groundwater conditions on their development.

To explore the origin of the dunes in the BJD, we conducted deep drilling in the southern desert to examine the underlying terrain of dunes. A water transport model of the unsaturated zones was used to determine the maintenance process of groundwater in the sand dunes. In addition, based on water table, TDS, and temperature of the basin groundwater, we identified the groundwater circulation process between dunes and basins. The results might provide a new understanding of the formation mechanism of high dunes and groundwater circulation modes.

2 Materials and methods

2.1 Study area

The BJD is located in western Inner Mongolia Autonomous Region, China, to the southwest of which is the Hexi Corridor and Qilian Mountains. The dominant wind direction in the desert is northwest, and driven by winter monsoon system of the Siberian High. Precipitation in the desert decreases from southeast to northwest, with summer precipitation accounting for more than 60% of annual precipitation (Wang et al., 2013; Dong et al., 2016). Limited precipitation observations in the BJD have shown that desert precipitation was prioritized over light rain (over 90%

precipitation events <5 mm) (Wang et al., 2013; Ma et al., 2014). Annual precipitation in the surrounding areas has provided references for the BJD, and Alagxa Right Banner to the south, Yabrai Town to the southeast, and Guaizihu Village to the north was 115.4, 90.1, and 42.9 mm/a, respectively (Ma et al., 2011). Regional evaporation intensified from southeast to northwest, and evaporation in the northwest of the desert was as high as 3000.0–4000.0 mm/a.

Since the Yanshan Movement, some mountains and basins have formed on the southern edge of the Alxa Plateau, such as Longshoushan Mountains, Beida Mountains, Yabrai Mountains, and the Ejin Depression Basin (Yan et al., 2001). The terrain of the BJD generally slopes to northwest. Elevation of southeastern desert near Yabrai Mountains reaches 1800 m, while that of the northwestern desert close to Guaizihu Village is only 900 m (Fig. 1a). Spatial development of the dunes changed from simple dunes in northwestern BJD to complex mega-dunes in southeastern BJD (Dong et al., 2009). The height of the Nortu mega-dunes is 500 m (relative height) in the southeastern BJD, which is the tallest dune in the world (Yan et al., 2001). Nortu Lake is the largest lake among 77 permanent lakes in the desert, with an area of approximately 1.5 km^2 and the maximum depth of 16 m (Yang, 2000; Wu et al., 2014).

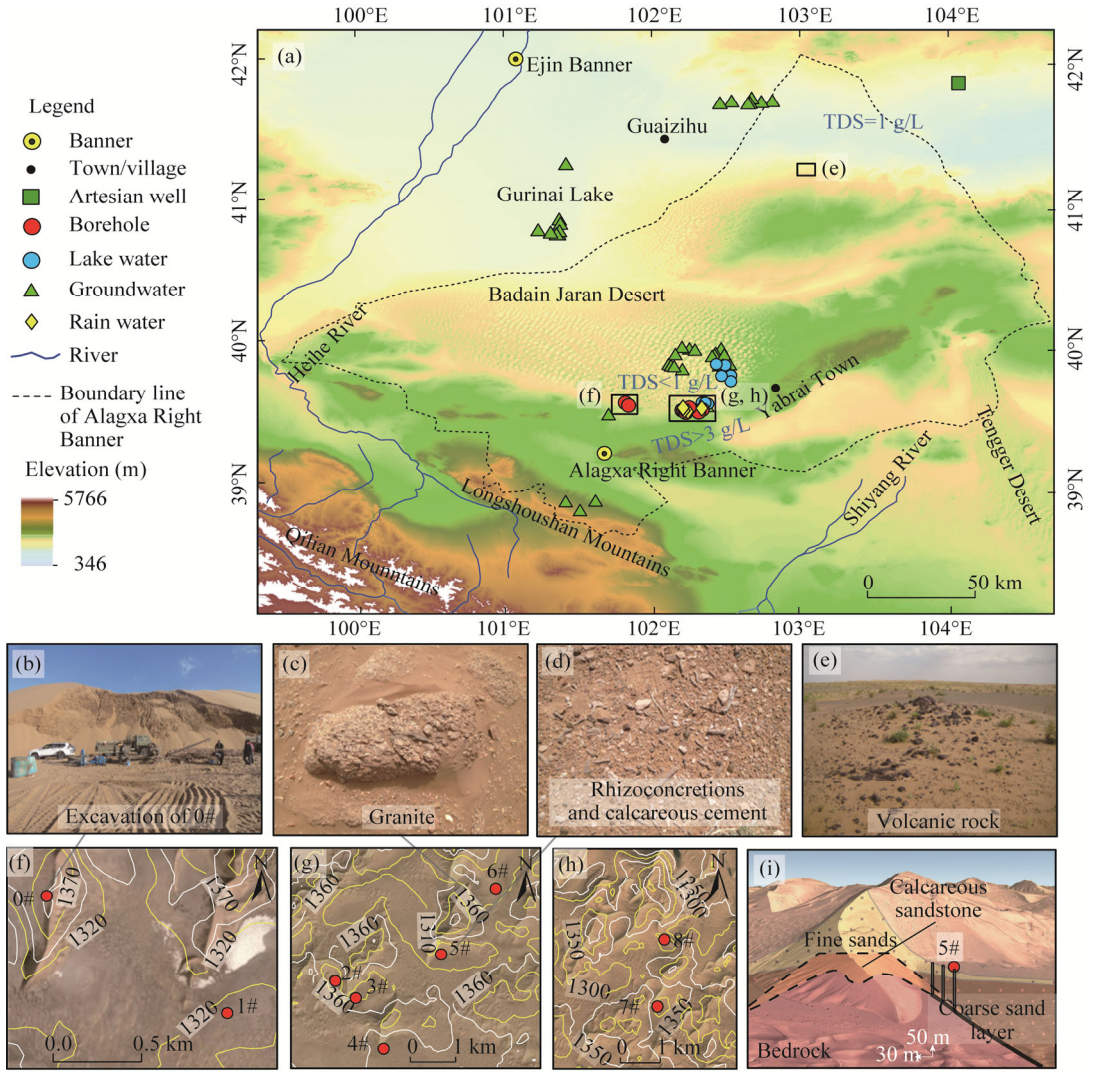

Fig. 1 Location map of study area. (a), location of the Badain Jaran Desert (BJD) and sampling distribution; (b), sand dune excavation site; (c)–(e), field discovery; (f)–(h), sampling dunes; (i), inner structure of inter-dune basin 5# and the black rectangles are the drill holes. TDS, total dissolved solutes. Gurinai Lake is a dry lake.

Given the lacustrine facies and sedimentation, desert surface is covered with Quaternary sediments of a certain thickness, even over 200 m (Yan et al., 2001). Therefore, to date, there have been relatively few geological investigations inside the BJD, and the underlying layer has not yet been examined. According to field investigations, relatively dense perennial herbaceous plants grow on the sand dunes, with granite exposed at the edge of basin and rhizoconcretion found in some lacustrine basins (Chen et al., 2006; Jiang and Chen, 2015) (Fig. 1c and d). Therefore, it was assumed that abundant groundwater exists here. In addition, volcanic debris was found scattered in some basins and near the top of dunes. Therefore, craters should have been present under dunes.

2.2 Field sampling

Boreholes were located at the southern margin of the BJD (Fig. 1f–h). One borehole was drilled in dune 0# and the other boreholes were drilled in inter-dune basins 1#–8#. The elevation of dune 0# is 1400 m. To facilitate drilling, we dug out a platform on the side of dune at an elevation of 1365 m with a drilling depth of 203 m (Fig. 1a). Surface elevation of boreholes ranges from 1264 to 1365 m, and the depth of boreholes ranges from 100 to 260 m (Table 1). Two additional exploration holes (inter-dune basins 5-1# and 5-2#) were drilled near the borehole 5#, and the terrain is shown in Figure 1i. Groundwater in the aquifer must be recovered for more than 48 h after pumping test to ensure groundwater flow stability. Probe was used to measure the temperature from groundwater level in the borehole at an interval of 1 m.

Table 1 Basic information of sampling boreholes

Borehole number	Longitude	Latitude	Surface elevation (m)	Drilling depth (m)	Depth of groundwater (m)
0#	101°48′42″E	39°33′58″N	1365	203	120.0
1#	101°49′51″E	39°33′36″N	1334	200	118.5
2#	102°12′01″E	39°31′28″N	1299	142	28.3
3#	102°12′35″E	39°31′22″N	1308	135	35.0
4#	102°12′54″E	39°30′42″N	1326	96	34.4
5#			1304	140	41.4
5-1#	102°13′42″E	39°31′47″N	1307	90	-
5-2#			1310	60	-
6#	102°14′16″E	39°32′33″N	1264	135	34.5
7#	102°18′26″E	39°30′53″N	1331	168	33.2
8#	102°19′47″E	39°31′35″N	1302	260	83.5

Note: -, no value.

Water samples were collected from 2006 to 2014, including 47 wells water, 27 desert groundwater samples, 21 groundwater samples in surrounding areas, 9 lake water samples, and 4 rain water samples (located near inter-dune basins 2#, 6#, and 8#). The locations are shown in Figure 1b. The samples were washed 3 times by original water, and sealed in polyvinyl chloride sample bottles. Hydrogen and oxygen isotope analysis was carried out by MAT253 (Thermo Fisher–Finnigan, Waltham, Massachusetts, USA) at the State Key Laboratory of Hydrology, Water Resources and Hydraulic Engineering, Hohai University, Nanjing. The test results are expressed as per thousand (‰) deviation from the isotopic composition of the Vienna standard seawater with the accuracy of $\delta^{18}O$ better than 0.1‰ and δD better than 2‰.

2.3 Water vapor transport model

Under drought conditions with relatively low precipitation, previous evaporation monitoring and simulated precipitation experiments have shown that heavy precipitation cannot penetrate into the dune interior (Ma et al., 2014; Dong et al., 2016). During the excavation of dune 0#, the wet sand inside the dune was visible (Fig. 1b), which raised the question of how groundwater migrates

upwards in the unsaturated zone of dunes. For dunes with relatively deep groundwater, it is not easy to analyze water migration through real-time monitoring of parameters, such as humidity and water content. Therefore, water transport model under deep aquifers proposed by Assouline and Kamai (2019) was used to simulate groundwater transport, which considers deep groundwater as the only source of water transport, and water only flows upward. Under this condition, hydraulic connectivity was bounded by evaporation front, under which the migration was dominated by liquid water. At evaporation front, fluxes of the liquid (q_l) and vapor-phases (q_v) are equal (Sadeghi et al., 2012). Relationship between them and d_{EF} (distance from the groundwater level to the evaporation front) is expressed as follows:

$$d_{EF} = \int_0^{h_r} \frac{1}{1 + q_l / K(h)} dh, \tag{1}$$

$$q_v = D \frac{-1}{\rho_w} \frac{\Delta c}{d_{WT} - d_{EF}}, \tag{2}$$

where d_{EF} is the distance from groundwater level to evaporation front (m); h_r is usually taken as $-\infty$ (m); q_l is the flux of liquid (m/s); $K(h)$ is the hydraulic conduction function of water head (m/s); d is the differentiation; h is the pressure head (m); q_v is the vapor-phase (m/s); D is the diffusion of water vapor in porous media (m^2/s); ρ_w is the density of water (kg/m^3); Δc is the variation of volumetric water vapor concentration between evaporation front and surface (kg/m^3); and d_{WT} is the distance from groundwater level to surface (m). Condensation amount of water vapor through unsaturated zone was measured by the method of Assouline and Kamai (2019).

$$K(h) = K_r \times K_s, \tag{3}$$

$$K_r = S_e^l \left[1 - \left(1 - S_e^{\frac{1}{m}} \right)^m \right]^2, \tag{4}$$

where K_r is the relative hydraulic conductivity; K_s is the saturated hydraulic conductivity (m/s); m and l are the fitting parameters; and S_e is the effective saturation, defined by:

$$S_e = \frac{\theta - \theta_r}{\theta_s - \theta_r}, \tag{5}$$

where θ is the volumetric moisture content (%); and θ_r and θ_s are the residual water content and saturated water content (%), respectively. The function of van Genuchten (1980) for the water retention is as follows:

$$S_e = \left(1 + |\alpha|^n\right)^{-m}, \tag{6}$$

where α (m^{-1}) and n are the fitting parameters.

Relationship between θ and h is determined by soil water retention curve. Water retention function is often used to describe soil-water transport in unsaturated porous media (Lebeau and Konrad, 2010). Aeolian sand of dunes is relatively uniform, and sand layer contains almost no clay particles (Zhao et al., 2011). Soil parameters are listed in Table 2. According to a grain size study of surface sediments, tall dunes have similar grain size parameters despite locating at different sites (Qian et al., 2011; Wei et al., 2022). Therefore, parameters selected in this study are representative.

3 Results

3.1 Sampled dunes and strata in the BJD

Grain sizes of sediments at different depths in the dunes and basins were compared. Particle size of aeolian sand in the dune was relatively uniform and mainly ranged from 0.150 to 0.250 mm, accounting for more than 75% of the strata, which contrasted with sediments in basins (Fig. 2a). Coarse sand content >1.000 mm increased significantly in the sediments of basins (Fig. 2a),

Table 2 Soil parameters adopted and corresponding results

Soil	α (m^{-1})	n	l	K_s	θ_r (%)	θ_s (%)	d_{EF} (m)
Sand*	8.60	2.14	0.5	2558	2.0	37.6	5.97
Fine	2.15	4.50	0.5	3285	3.4	42.0	<1.00

Note: parameters with * is referenced from Assouline et al. (2013). α, n, and l, fitting parameters; K_s, saturated hydraulic conductivity; θ_r, residual moisture content; θ_s, saturated water content; d_{EF}, distance from groundwater level to evaporation front.

which were mainly granite weathering products. Based on the drilling results for dune 0#, in the dune with a height of 100 m, the thickness of overlying aeolian sand layer reached 94 m, including 20 m removed for the platform. Calcareous sandstone occurred at a depth of 74–190 m, where sand particles were identical to those in the upper layer. At a depth of 190–203 m, the saturated coarse sand layer contained red clay, the main components of which were Fe_2O_3 and Mn_2O_3. Granite bedrock was encountered at a depth of 200 m. Boreholes of inter-dune basins 1#–8# were in different basins. Some boreholes (inter-dune basins 2#–7#) were near the foot of different dunes rather than in the center of each basin and stratigraphic compositions of them were similar. They mainly consisted of coarse sand and gravel layers with high permeability. The three drilling holes (inter-dune basins 5-1#, 5-2#, and 5#) located in the same basin showed granite at elevations of 1250, 1217, and 1164 m, with horizontal distances from the dune foot of 30, 60, and 90 m, indicating that granite uplift slope reached 1.43 (55°) (Fig. 1i; Table 1). Surface slope distribution in southern part of the BJD showed that the slope of dunes usually ranged from 0° to 30° (Fig. 2c and d). Therefore, uplift of the bedrock contributed to the height of mega-dunes.

Volcanic clasts were found at different depths in sedimentary boreholes, which likely washed into basins from crater along with weathered particles. Therefore, volcanic eruptions likely occurred before desert formation. Eruption penetrated granite basement and created an undulating landscape as confirmed by drilling. Since the Cenozoic era, magmatic activity has occurred in the

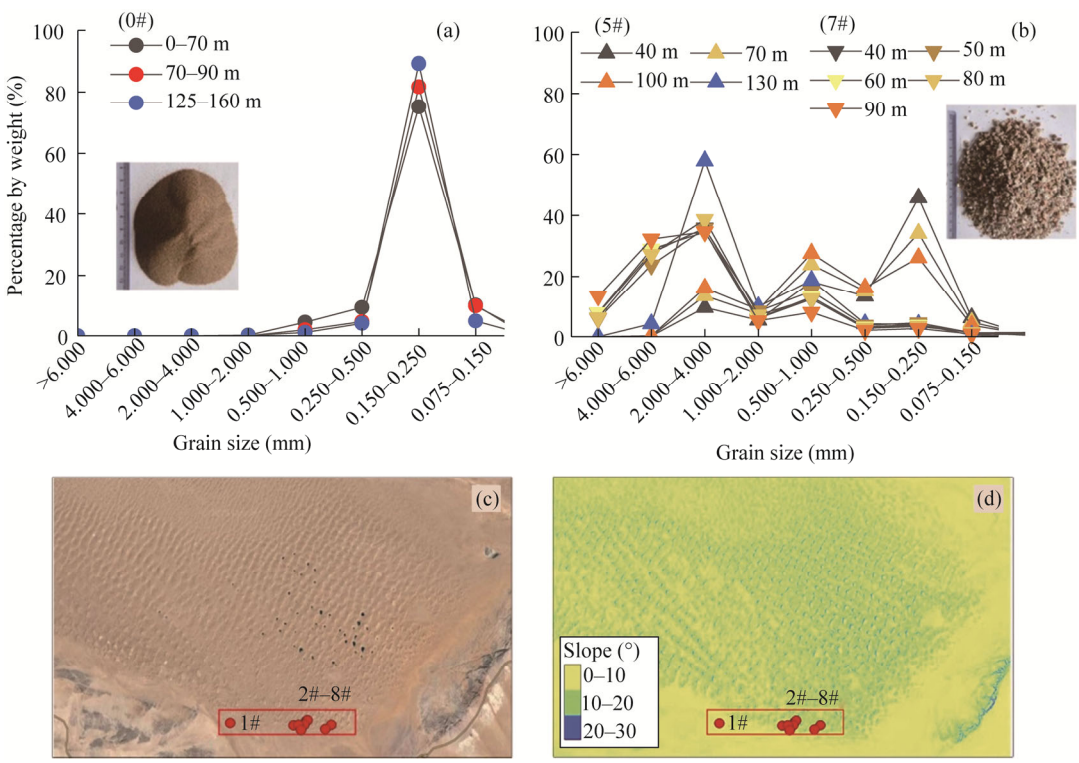

Fig. 2 Grain size gradation of dune 0# (a), and inter-dune basins 5# and 7# (b). (c), field image; (d), slope of sand dunes in southern BJD.

Alagxa Plateau, which may have resulted in the uplift of underlying granite.

Previous BJD surveys assumed that sand dunes and basins were all covered by aeolian sand, even with a thickness of more than 200 m. While the basin boreholes near southern margin of the desert had granite at depths of 90–100 m, some were exposed at the edge of the basin (Fig. 1d). Previous hydrogeological holes were drilled in the center of the basin, similar to borehole of inter-dune basin 8#, at a depth of 260 m with exposed argillaceous sandstone at the bottom, which was approximately 100 m thick. This difference depends on the distance between borehole and dunes.

3.2 Groundwater movement in dunes

Based on simulation, we found that evaporative front located at a depth below 6 m, demonstrating that upward movement of water in the aeolian sand layer for nearly 100 m does not have continuous hydraulic conductivity. Therefore, height of the capillary water is limited (Fig. 3). Above evaporative front, water phase changes to vapor and migrates as it diffuses to the surface. When water vapor migrates in the aeolian sand layer through diffusion, saturated water pressure of water vapor migrates accordingly owing to temperature difference of aeolian sand layers at different depths; therefore, more water vapor than saturated water pressure will condense (Fig. 3). However, the amount of condensed water formed by upward movement of water was relatively small (Fig. 3). With deep groundwater table of dunes, thin-film water and water vapor migration are the main forms of groundwater migration.

After rainfall of the desert, moisture content of sand layer at a depth >1 m was not significantly different from that of sand layer without long-term precipitation (Fig. 4). This indicates that there should be a balance between evaporation and condensation in dunes. Although water content in basins can reach 6% after rainfall, it was usually less than 3% at a depth >1 m. Unless water table was very high, water content of basins as a whole was lower than those of dunes.

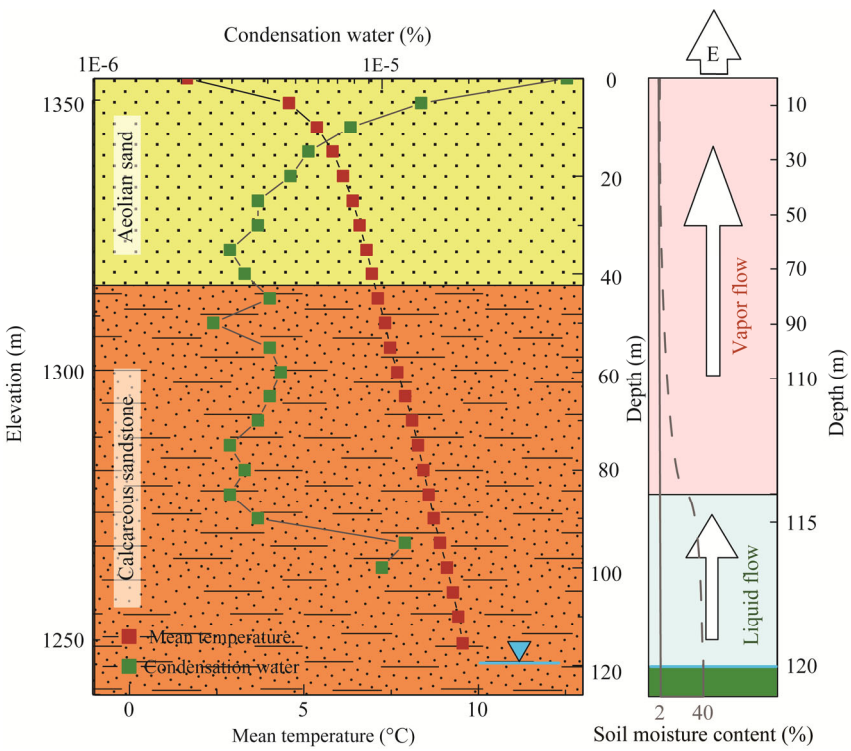

Fig. 3 Formation composition of dune 0# and conceptual water migration in vadose zone, modified from Assouline and Kamai (2019). Blue inverted triangle and line indicate groundwater level. E, evaporation. Blue inverted triangle and line indicate groundwater level.

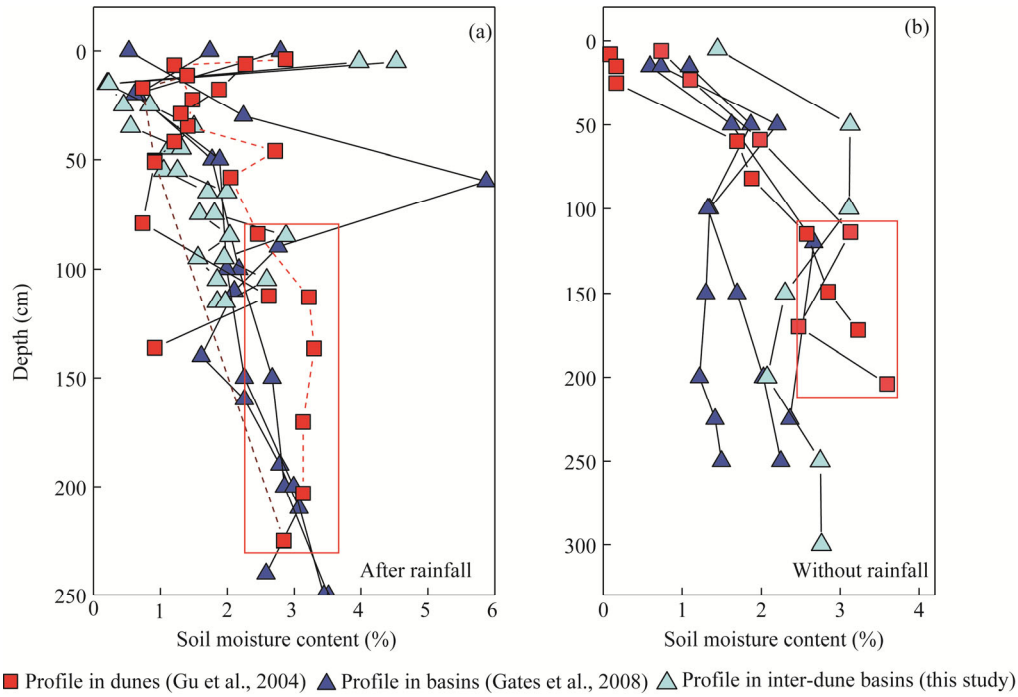

Fig. 4 Profile of soil moisture content in dunes and basins of the Badain Jaran Desert (BJD). (a), soil moisture content after rainfall, (b), soil moisture content without rainfall over a long time. Water content of dunes in the two red boxes are in the ranges of 3%–4%.

3.3 Groundwater characteristics of basins

Pumping test results showed that recharge from dunes was abundant and stable. Pumping flow of inter-dune basins 1#–6# and 8# were more than 20 m^3/h; and drilling potential was more than 3.40×10^6 m^3/a (Fig. 5a). Water levels and TDS of inter-dune basins 2#–8# were compared, because distances between them were relatively small. If there is a flow and recharge relationship between groundwater in different basins, it can be identified as water flows from high to low water levels and TDS increases along flow path. It can be seen that inter-dune basins 4# and 3#, and inter-dune basins 5# and 6# may have recharge relationships (Fig. 5b). However, during pumping period for inter-dune basin 3#, there was no change in water level at inter-dune basin 4#. In a similar range of borehole depths, temperature of inter-dune basin 5# was nearly 2°C lower than that of inter-dune basin 6# (Fig. 5c). Considering that ground temperature below a depth of 30 m is almost unaffected by solar radiation, groundwater temperature difference in different basins should be a result of recharge. Therefore, basin groundwater recharge is relatively independent.

Results of isotope analysis showed that snowmelt in the Qilian Mountains was the source of groundwater in the BJD. Isotopic compositions are shown in Figure 5d. $\delta^{18}O$ and δD of well water samples ranged from –6.83‰ to –2.41‰ and from –65.40‰ to –39.20‰, respectively. $\delta^{18}O$ and δD of groundwater in desert hinterland ranged from –6.57‰ to –2.30‰ and from –73.60‰ to –45.10‰, respectively, which formed an evaporation line (EL) ($\delta D= 4.63\delta^{18}O–32.31$) with $\delta^{18}O$ and δD (from –63.60‰ to 14.4‰ and from –5.66‰ to 9.69‰, respectively) of desert lake water samples. $\delta^{18}O$ and δD of soil water near EL indicates water migration from groundwater to sand layer. $\delta^{18}O$ (–82.8‰ to –14.3‰) and δD (–9.8‰ to 11‰) of groundwater in area of northwestern BJD (Gurinai Lake and Guaizihu Village) indicates that here is desert groundwater discharge area. While $\delta^{18}O$ and δD of groundwater at the foot of Longshou Mountains ranged from –10.58‰ to –8.91‰ and –74.3‰ to –58.6‰, respectively, following the LMWL. Intersection point (–12.55‰ and –90.44‰) between EL and global meteoric water line (GMWL) is more depleted than desert rainfall but similar to snowmelt in the Qilian Mountains, indicating actual recharge.

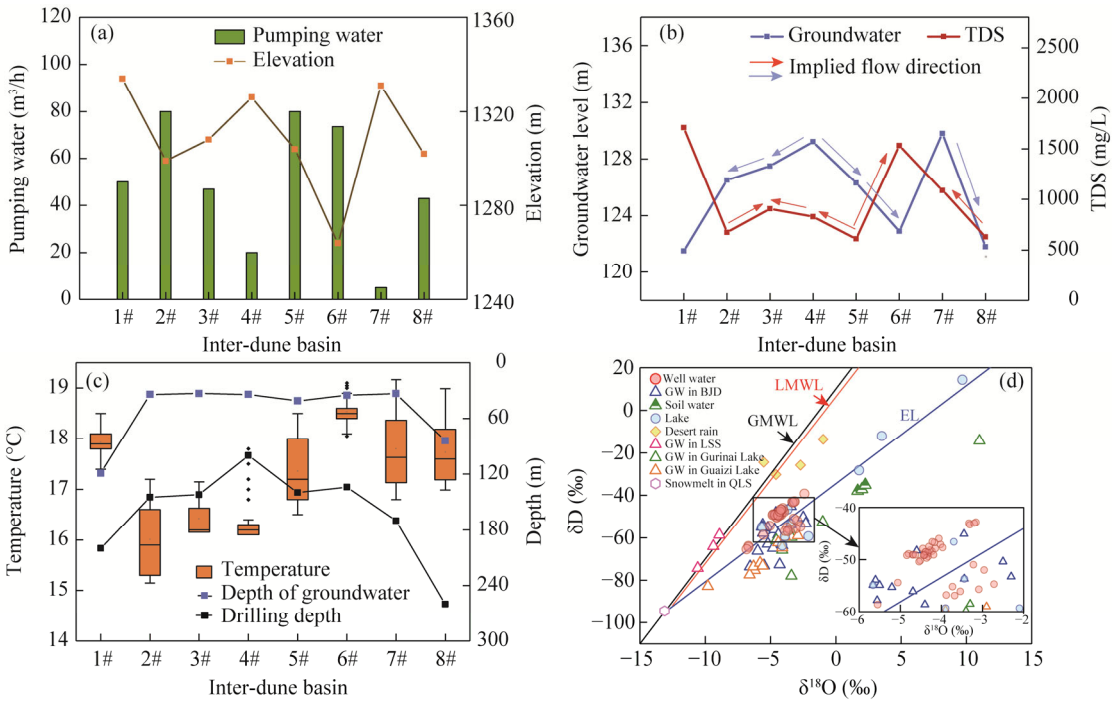

Fig. 5 Groundwater (GW) of inter-dune basins in the Badain Jaran Desert (BJD). (a), pumping water and elevation; (b), groundwater level and total dissolved solids (TDS); (c), temperature and depth; (d), relationship between δD values. In Figure 5c, boxes indicate the IQR (interquartile range, 75th to 25th of the data). The median value is shown as a line within the box. Outlier is shown as black circle. Whiskers extend to the most extreme value within 1.5×IQR. Isotope data of soil water in Figure 5d are referenced from Chen et al. (2012), local meteoric water line (LMWL) is referenced from Jin et al. (2018), and snowmelt data are referenced from Ren (1999). GMWL, global meteoric water line; LSS, Longshou Mountains; QLS, Qilian Mountains; EL, evaporation line.

4 Discussion

4.1 Effects of wind and bedrock on dune formation

Wind mainly controls the formation and shapes of dunes, which are almost all northwest-oriented. As wind intensity will affect the evaporation amount in unsaturated zone of dunes, moisture content of sand layer will decrease when evaporation amount is less than condensation amount, thus becoming a dry sand layer. Thickness of dry sand layer is also related to wind intensity. Wind on the windward slope is relatively stronger and it carries away more particles, so the thickness of dry sand layer is thinner. However, wind has no significant contribution to the dunes' height (Dong et al., 2009; Yang et al., 2011; Meng et al., 2022). Under wind dominance, dust should cover the bedrock evenly or fill in depression areas. If dunes were formed only by wind, there would be no basin. Actually, dunes in the BJD have gradually converged to composite ridge shaped mega-dunes with a height of nearly 500 m (Yan et al., 2001), while basins are only covered with aeolian sand at a certain thickness (1 m) on the surface. This leads to the question of why aeolian sands accumulate on dunes rather than in basins. Dune height setting is more complex (Gunn et al., 2022). Size of sand particle gradually increased from dunes to basins (Fig. 2a and b). Therefore, dunes cannot form in desert basins because coarse-grained layer deposited in the desert basins prevents the upward migration and recharge of thin-film water. Accumulation of aeolian sand in basins can only form temporarily moving dunes owing to the lack of groundwater support. Water can increase the cohesion between sand particles to resist wind erosion, and sand dunes can continuously accumulate (Chen et al., 2004). Groundwater should be present under dunes to maintain sand accumulation.

Some studies have also speculated that fluctuation in the underlying bedrock of sand dunes may affect the flow of surface aeolian sand (Wang, 1990; Yang, 2000; Chen et al., 2006). However, according to gravity data, the shape of underlying bedrock does not completely match that of sand dune completely (Yang et al., 2011). Slope of dune surface was actually greater than that of bedrock, indicating that the height of dune is mainly dependent on calcareous sandstone and aeolian sand deposit. Calcareous sandstone was regarded as "skeleton" of dunes (Qian and Liu, 2015). Surface around dunes is also littered with rhizoconcretions and calcareous cements, which are widespread in the BJD (Dong et al., 2013), and many lakes exist travertine in springs.

Obviously, deposition of calcium carbonate was not caused by evaporation. Regarding the source of calcium carbonate, Yan et al. (2001) and Yang (2011) believed that abundant precipitation in a humid climate would dissolve calcium carbonate in the strata and mix it with groundwater. Later, calcium carbonate precipitated owing to decrease in groundwater level in an arid climate. However, this hypothesis had no corresponding geochemical analysis (Yang, 2000; Yang et al., 2011). If calcareous sandstone was created in this humid climate, presence of abundant groundwater and its storage space inside the sand dune could not be explained. Chen et al. (2006) reported that calcium carbonate derived from confined water. Given that the solubility of calcium carbonate increases with the pressure of water, calcium carbonate in deep groundwater has high solubility (Chen et al., 2004), which decreases when groundwater glows out of surface, forming calcium carbonate precipitation (Chen et al., 2006). Moreover, $^{87}Sr/^{86}Sr$ (Strontium) values of groundwater in the BJD were similar to those of marine sedimentary carbonate rocks, which indicated that calcareous sandstone layer and calcium carbonate particles in the sediments were related to deep groundwater (Chen and Jiang, 2015). Large number of calcium ions carried by deep-circulation groundwater gradually formed a calcareous cement layer and rhizoconcretions in sand dunes. Therefore, fixed mega-dunes can resist wind erosion, accumulate, and grow.

4.2 Groundwater formed dunes

Wet sand layers inside dunes are in sharp contrast to arid climate of the BJD (Zhu, 2023). Meanwhile, lee slopes of sand dunes are greater than angle of repose of sand (34°), even up to 45° (Yan et al., 2001). Experiments have shown that angle of repose increases to 65° with a moisture content of up to 4.7%, indicating that high water content of sand layers increase the ability of dunes to resist wind erosion (Webster, 1919; Chen et al., 2004). Zhao et al. (2017) highlighted that heavy precipitation can infiltrate owing to infiltration-excess runoff. According to mechanism analysis of formation of infiltration-excess runoff, precipitation intensity needs to be greater than infiltration intensity of sand layer for penetration. However, observed precipitation intensity in desert was significantly lower than infiltration rate of sandy layer (about 20 mm/min) (Wang et al., 2013).

For dunes, potential evaporation is substantially greater than actual evaporation (Wang et al., 2013; Ma et al., 2014); actual evaporation is determined by precipitation (Liu et al., 2009; Hu et al., 2015). Limited precipitation and evaporation observations showed that precipitation event in the BJD was given priority over light rain (over 90%<5 mm). Theoretically, infiltration precipitation should be absorbed on the surface of soil particles and form a thin-film water layer owing to soil surface charges (Gong et al., 2018). Only when water content of dry sand layer reaches the maximum water-holding capacity can the water become gravity water and continue to penetrate wet sand layer (Dong et al., 2016). Water content of sand layer is usually 3%–4%, which does not reach the maximum water-holding capacity (5%), even after precipitation (Gu et al., 2004). This indicates that precipitation has a limited effect on soil moisture content in dunes (Fig. 4). All atmospheric precipitation evaporated from mega-dunes approximately one day after this type of precipitation (Ma et al., 2014). Therefore, wet layer should form via groundwater vapor transport.

Given that air temperature of dune 0# was measured in winter, simulated condensed water volume was larger than those in other seasons. Therefore, it is likely that sand dunes were more

likely to have developed rapidly during the period when groundwater temperature was high, rather than under modern conditions. Elevation of calcareous sandstone also indicates that water table in the past was substantially higher than that at present. According to grading data for sand dunes, particle size of aeolian sand is mainly 0.15–0.25 mm, and the porosity is approximately 40%. Therefore, water content can reach 3% when film water is up to 3 nm, approximately equal to current moisture content of wet sand layer inside mega-dunes (2%–4%). Therefore, water in sand dunes should be stored as thin-film water, which is important in unsaturated zones of arid areas (Lebeau and Konrad, 2010). Previous studies on water vapor in unsaturated zone in the BJD have mainly focused on basins with a groundwater depth of ≤5 m, which is within the range of capillary water transport. Meanwhile, to date, few studies have focused on water migration in unsaturated zone with a deep groundwater table. Through simulation of water migration in dunes, groundwater moved upward in the form of capillary water and water diffusion, accompanied by countless evaporation and condensation. Currently, groundwater can exist in the form of thin-film water, evaporation, and condensation. Condensation can increase the cohesion between aeolian particles. When surface evaporation of dunes is greater than that of condensed water, sand will be blown away by wind.

Formation and evolution processes of dunes mainly involve two steps, first, aeolian sand layer resists wind erosion under action of condensate water, which form via condensation after moving from groundwater. Second, as $CaCO_3$-rich groundwater gushes out, calcium carbonate precipitate and aeolian sand are cemented into sandstone by calcium, becoming a hard "core". It is likely that there are two stages of dune growth. At the beginning, groundwater temperature is relatively high, water vapor migrates rapidly, and a large amount of aeolian sand accumulates on the surface. When water temperature decreases, water vapor migration in unsaturated zone slows, amount of water is lower, and dune enters a slow maintenance period.

4.2 Groundwater source of dunes

This is the first attempt to discover groundwater source inside dunes in the BJD, thus confirming the significant effect of groundwater on the development of sand dunes. Discovered shallow runoff indicates that groundwater in dunes flowed into basins (Zhao et al., 2017). Elevation of calcareous sandstone in dune 0# was higher than that of calcareous mudstone in adjacent basin (inter-dune basin 1#), indicating that dune 0# should be upstream of groundwater. Gravity data also indicated the presence of higher water levels in mega-dunes than in surrounding lakes (Yang et al., 2011). However, drilling in dunes has not revealed abundance of groundwater. This is because carbonate concentration of carbonate in groundwater was substantially higher than its saturation concentration. Supersaturated carbonates deposit calcium carbonate in the pores of sand grains, cementing e aeolian sand with calcareous sandstone. Permeability coefficient of sandstone is less than 1×10^{-3} m/d, significantly less than that of aeolian sand (2.47 m/d) (Cheng et al., 2010). Therefore, flow of dune 0# was relatively low. Groundwater in dunes should flow mainly in sandstone fissure. In contrast, inter-dune basins, as natural reservoirs, can easily obtain abundant groundwater.

Groundwater in dunes may be come from basalt-sourced groundwater, which can be replenished through crater and maintain a large flow during dry season (Jia et al., 1993; Chen and Jiang, 2015; Jiang and Chen, 2015). Basalt-sourced groundwater is a product of volcanic activity and differs from pore, fissure, and karst waters. Storage and flow of groundwater depend on the development of secondary basaltic pores (Kulkarni et al., 2000). As lava flows increase, the primary porosity, joints, and secondary fissures gradually form a complete water transport and storage system (Jia et al., 1993). According to the composition of material elements, desert groundwater is rich in Sr (0.54–1.02 mg/L), which exceeds the mean value of rivers around desert (Liu et al., 2016). Measured contents of H_2SiO_3 and CO_3^{2-} were both high, which is consistent with that of basalt groundwater (Jia et al., 1993; Chen and Jiang, 2015; Ma et al., 2022). Combined with the existence of crater under sand dunes, it is speculated that relatively independent water channel is below crater (Fig. 6).

In the early stages, temperature of groundwater upwelling from volcanic craters should be high. Next, a significant amount of water vapor diffused into atmosphere and condensed in surface and sand particles brought by wind were stuck, continuously accumulating to form sand dunes. Shape of sand dunes indicates the direction of groundwater flow (Fig. 6). When groundwater supply was sufficiently high, a symmetrical lake formed at the end of sand dunes. Currently, groundwater from sand dunes can gather in basins, which acts as a natural reservoir. However, during runoff, groundwater dissolves salt in sediments, so drilling in the area closer to dunes can obtain higher quality groundwater resources.

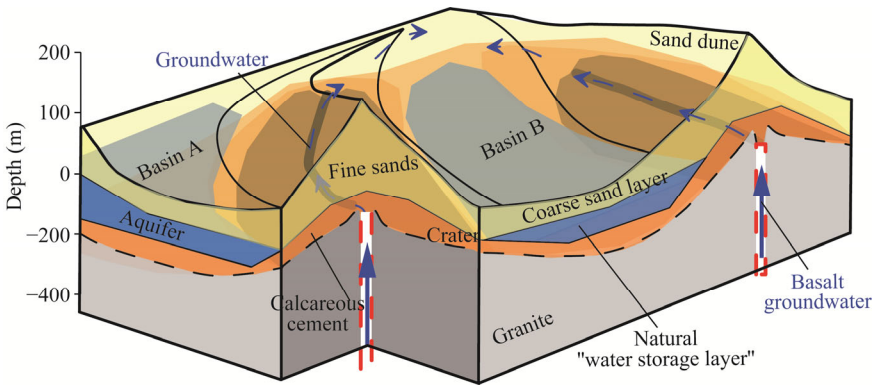

Fig. 6 Structure of sand dune and inter-dune basin with a conceptual diagram of groundwater flow. Basins A and B are separated by granite uplift and receive independent groundwater recharge from crater under dunes.

Affected by harsh environment of the BJD, this study was conducted at the southern edge of desert, and the role of groundwater was emphasized in the analysis of formation mechanism of sand dunes. Shape of mega-dunes in the desert hinterland is relatively more complex, with simple sand dunes piled up on top of windward slope; however, there is still a large gap in the hydrogeological survey of mega-dunes there. Results of water transport model are only for reference, because parameters were obtained from related studies. Also, for an arid area with an aquifer depth greater than 100 m, water migration process in the unsaturated zone requires further research to provide a more systematic theoretical study of mega-dunes' formation mechanism. Meanwhile, groundwater resources in the hinterland of desert are also noteworthy because water storage only in the eight inter-dune basins in southern margin has reached 3.40×10^6 m^3/a. Mega-dunes in the hinterland are often accompanied by larger lakes and even freshwater lakes (Dong et al., 2013; Zhu, 2023). Height of sand dunes is proportional to the amount of groundwater and area of lakes, which implies that water resources in sand dunes in desert should be more abundant.

This study not only reveals a new pattern of dune growth by examining the formation of world's tallest dune but also provides insights into water cycle in desert for other arid areas to exploit water resources. Wet sand layers, calcareous sandstone, and perennial grass occur in many desert dunes worldwide (Grandjean et al., 2001; Lancaster et al., 2002; Hesse, 2011), and groundwater in deserts is irreplaceable source for regional drinking water (Edmunds et al., 2003; Hakimi et al., 2021). Understanding groundwater recharge, runoff, and discharge processes can provide a theoretical basis for obtaining high-quality water resources.

5 Conclusions

Compared with deserts in other arid areas, the BJD has developed the tallest dune worldwide (nearly 500 m), with a general height of 200–300 m, which is maintained by groundwater. Deep drilling in dunes and different inter-dune basins were conducted to explore the formation mechanism of sand dunes in the BJD, revealing that elevation between dunes and basins was

mainly caused by aeolian sand accumulation. Water migration simulation showed that water connectivity was limited and that water migration was mainly based on vapor diffusion. Water in sand dunes should be stored as thin-film water, and amount of evaporation and condensation determines whether sand dunes will be eroded by wind. Uplift of granite beneath dunes resulted in no unified hydraulic connections among different basins, which received an independent supply through carter below dunes. Moreover, as natural reservoirs, it is easier for basins to obtain abundant groundwater. This study provides direct geological information on the formation mechanism of sand dunes, a new perspective for studying the relationship between dunes and lakes, and a theoretical basis for the allocation of water resources in arid areas.

Conflict of interest

The authors declare that they have no known competing financial interests or personal relationships that could have appeared to influence the work reported in this paper.

Acknowledgements

This work was funded by the National Natural Science Foundation of China (61771183). The authors are grateful for the help of Mr. SU Zhiguo for isotopic analyses of samples.

Author contributions

Conceptualization: CHEN Jiaqi, CHEN Jiansheng; Methodology: MA Xiaohui; Formal analysis: CHEN Jiansheng, WANG Wang; Writing - original draft preparation: WANG Wang; Writing - review and editing: WANG Tao, ZHAN Lucheng, ZHANG Yitong; Funding acquisition: CHEN Jiaqi; Supervision: CHEN Jiansheng.

References

Assouline S, Kamai T. 2019. Liquid and vapor water in vadose zone profiles above deep aquifers in hyper-arid environments. Water Resources Research, 55(5): 3619–3631.

Assouline S, Tyler S W, Selker J S, et al. 2013. Evaporation from a shallow water table: Diurnal dynamics of water and heat at the surface of drying sand. Water Resources Research, 49(7): 4022–4034.

Bai Y, Wang N, Liao K, et al. 2011. Geomorphological evolution revealed by aeolian sedimentary structure in Badain Jaran Desert on Alxa Plateau, Northwest China. Chinese Geographical Science, 21: 267–278.

Chen J, Li L, Wang J, et al. 2004. Groundwater maintains dune landscape. Nature, 432: 459–460.

Chen J, Zhao X, Sheng X, et al. 2006. Formation mechanisms of megadunes and lakes in the Badain Jaran Desert, Inner Mongolia. Chinese Science Bulletin, 51: 3026–3034.

Chen J, Jiang Q. 2015. Research progress of ground water deep circulation. Water Resources Protection, 31(6): 8–17, 66. (in Chinese)

Cheng D, Wang W, Li W, et al. 2010. The unsaturated hydraulic parameters for aeolian sand. Agricultural Science & Technology, 11(10): 1–3. (in Chinese)

Dong C, Wang N, Chen J, et al. 2016. New observational and experimental evidence for the recharge mechanism of the lake group in the Alxa Desert, north-central China. Journal of Arid Environments, 124: 48–61.

Dong Z, Qian G, Luo W, et al. 2009. Geomorphological hierarchies for complex mega-dunes and their implications for mega-dune evolution in the Badain Jaran Desert. Geomorphology, 106(3–4): 180–185.

Dong Z, Qian G, Lv P, et al. 2013. Investigation of the sand sea with the tallest dunes on Earth: China's Badain Jaran Sand Sea. Earth-Science Reviews, 120: 20–39.

Edmunds W M, Guendouz A H, Mamou A, et al. 2003. Groundwater evolution in the continental intercalaire aquifer of southern Algeria and Tunisia: Trace element and isotopic indicators. Applied Geochemistry, 18(6): 805–822.

Gates J B, Edmunds W M, Ma J, et al. 2008. Estimating groundwater recharge in a cold desert environment in northern China using chloride. Hydrogeology Journal, 16: 893–910.

Gong Y, Tian R, Li H. 2018. Coupling effects of surface charges, adsorbed counterions and particle-size distribution on soil water infiltration and transport. European Journal of Soil Science, 69(6): 1008–1017.

Grandjean G, Paillou P, Dubois-Fernandez P, et al. 2001. Subsurface structures detection by combining L-band polarimetric

SAR and GPR data: Example of the Pyla Dune (France). IEEE Transactions on Geoscience and Remote Sensing, 39(6): 1245–1258.

Gu W, Chen J, Wang J, et al. 2004. Challenge from the appearance of vadose water within the surface layer of megadunes Badain Jaran Dune desert, Inner Mongolia. Advances in Water Science, 15(6): 695–699. (in Chinese)

Gunn A, Casasanta G, Di Liberto L, et al. 2022. What sets aeolian dune height? Nature Communication, 13: 2401, doi: 10.1038/s41467-022-30031.

Hakimi Y, Orban P, Deschamps P, et al. 2021. Hydrochemical and isotopic characteristics of groundwater in the Continental Intercalaire aquifer system: Insights from Mzab Ridge and surrounding regions, north of the Algerian Sahara. Journal of Hydrology: Regional Studies, 34: 100791, doi: 10.1016/j.ejrh.2021.100791.

Hesse P. 2011. Sticky dunes in a wet desert: Formation, stabilisation and modification of the Australian desert dunefields. Geomorphology, 134(3–4): 309–325.

Hu F, Yang X. 2016. Geochemical and geomorphological evidence for the provenance of aeolian deposits in the Badain Jaran Desert, northwestern China. Quaternary Science Reviews, 131: 179–192.

Hu W, Wang N, Zhao L, et al. 2015. Surface energy and water vapor fluxes observed on a megadune in the Badain Jaran Desert, China. Journal of Arid Land, 7(5): 579–589.

Jia F, Qin Z, Han Z. 1993. Basic characteristics of groundwater in basalt of China. Hydrogeology and Engineering Geology, 20(4): 30–32. (in Chinese)

Jiang Q, Chen J. 2015. Analysis on water balance of deep cycle groundwater supplying Tianchi Lake of Changbai Mountain. Water Resources Protection, 31(5): 7–13. (in Chinese)

Jin K, Rao W B, Tan H B, et al. 2018. H-O isotopic and chemical characteristics of a precipitation-lake water-groundwater system in a desert area. Journal of Hydrology, 559: 848–860.

Kulkarni H, Deolankar S B, Lalwani A, et al. 2000. Hydrogeological framework of the Deccan basalt groundwater systems, west-central India. Hydrogeology Journal, 8: 368–378.

Lancaster N, Kocurek G, Singhvi A, et al. 2002. Late Pleistocene and Holocene dune activity and wind regimes in the western Sahara Desert of Mauritania. Geology, 30(11): 991–994.

Lebeau M, Konrad J M. 2010. A new capillary and thin film flow model for predicting the hydraulic conductivity of unsaturated porous media. Water Resources Research, 46(12): W12554, doi: 10.1029/2010WR009092.

Liu B, Ma Z, Xu J, et al. 2009. Comparison of pan evaporation and actual evaporation estimated by land surface model in Xinjiang from 1960 to 2005. Journal of Geographical Sciences, 19: 502–512.

Liu W, Jiang H, Shi C, et al. 2016. Chemical and strontium isotopic characteristics of the rivers around the Badain Jaran Desert, northwest China: Implication of river solute origin and chemical weathering. Environmental Earth Sciences, 75: 1119, doi: 10.1007/s12665-016-5910-0.

Lorenz R D, Radebaugh J. 2009. Global pattern of Titan's dunes: Radar survey from the Cassini prime mission. Geophysical Research Letters, 36(3): L03202, doi: 10.1029/2008GL036850.

Luo X, Jiao J J, Wang X S, et al. 2016. Temporal 222Rn distributions to reveal groundwater discharge into desert lakes: Implication of water balance in the Badain Jaran Desert, China. Journal of Hydrology, 534: 87–103.

Ma F, Chen J, Zhan L, et al. 2022. Coastal upward discharge of deep basalt groundwater through developed faults: A case study of the Subei Basin, China. Journal of Environmental Management, 306: 114469, doi: 10.1016/j.jenvman.2022.114469.

Ma N, Wang N, Li Z, et al. 2011. Analysis on climate change in northern and southern marginal zones of Badain Juran Desert during 1960–2009. Arid Zone Research, 28(2): 242–250. (in Chinese)

Ma N, Wang N, Zhao L, et al. 2014. Observation of mega-dune evaporation after various rain events in the hinterland of Badain Jaran Desert, China. Chinese Science Bulletin, 59: 162–170.

Meng N, Wang N, Zhao L, et al. 2022. Wind regimes and associated sand dune types in the hinterland of the Badain Jaran Desert, China. Journal of Arid Land, 14(5): 473–489.

Parteli E J, Herrmann H J. 2007. Dune formation on the present Mars. Physical Review E, 76(4): 41307, doi: 10.1103/PhysRevE.76.041307.

Ping L, Narteau C, Dong Z, et al. 2014. Emergence of oblique dunes in a landscape-scale experiment. Nature Geoscience, 7: 99–103.

Qian G, Dong Z, Luo W, et al. 2011. Grain size characteristics and spatial variation of surface sediments in the Badain Jaran Desert. Journal of Desert Research, 31(6): 1357–1364. (in Chinese)

Qian R Y, Liu L B. 2015. Internal structure of sand dunes in the Badain Jaran Desert revealed by GPR. IEEE Journal of Selected Topics in Applied Earth Observations and Remote Sensing, 9(1): 159–166.

Ren J. 1999. A study of chemical characteristics of snow, precipitation and surface water in the basin of the glacier No. 29 in

Danghe Nanshan, Qilian Mountains. Journal of Glaciolgy and Geocryology, 21(2): 151–154. (in Chinese)

Sadeghi M, Shokri N, Jones S B. 2012. A novel analytical solution to steady−state evaporation from porous media. Water Resources Research, 48(9): 12060, doi: 10.1029/2012wr012060.

van Genuchten M T. 1980. A closed form equation for predicting the hydraulic conductivity of unsaturated soils. Soil Science Society of America Journal, 44(5): 892–898.

Wang N, Ma N, Chen H, et al. 2013. A preliminary study of precipitation characteristics in the hinterland of Badain Jaran desert. Advances in Water Science, 24(2): 153–160. (in Chinese)

Wang T. 1990. Formation and evolution of Badain Jaran Desert, China. Journal of Desert Research, 10(4): 29–40. (in Chinese)

Webster A G. 1919. On the angle of repose of wet sand. Proceedings of the National Academy of Sciences, 5(7): 263–265.

Wei G, Zhang C, Li Q, et al. 2022. Grain-size composition of the surface sediments in Chinese deserts and the associated dust emission. CATENA, 219: 106615, doi: 10.1016/j.catena.2022.106615.

Wu Y, Wang N, Zhao L, et al. 2014. Hydrochemical characteristics and recharge sources of Lake Nuoertu in the Badain Jaran Desert. Chinese Science Bulletin, 59: 886–895.

Yan M, Wang G, Dong G, et al. 2001. Study on mega dunes development and environmental change in Badain Jaran Desert. Journal of Desert Research, 21(6): 361–366. (in Chinese)

Yang X. 2000. Landscape evolution and precipitation changes in the Badain Jaran Desert during the last 30,000 years. Chinese Science Bulletin, 45(11): 1042–1047.

Yang X, Williams M A J. 2003. The ion chemistry of lakes and late Holocene desiccation in the Badain Jaran Desert, Inner Mongolia, China. CATENA, 51: 45–60.

Yang X, Ma N, Dong J, et al. 2010. Recharge to the inter-dune lakes and Holocene climatic changes in the Badain Jaran Desert, western China. Quaternary Research, 73(1): 10–19.

Yang X, Scuderi L A. 2010. Hydrological and climatic changes in deserts of China since the Late Pleistocene. Quaternary Research, 73(1): 1–9.

Yang X, Scuderi L, Liu T, et al. 2011. Formation of the highest sand dunes on Earth. Geomorphology, 135(1–2): 108–116.

Zhang Z, Liang A, Zhang C, et al. 2021. Gobi deposits play a significant role as sand sources for dunes in the Badain Jaran Desert, Northwest China. CATENA, 206: 105530, doi: 10.1016/j.catena.2021.105530.

Zhao J, Zhang C, Dong Z, et al. 2011. Particle size composition and formation of the mega-dune in the Badain Jaran Desert. Acta Geologica Sinica, 85(8): 1389–1398. (in Chinese)

Zhao J, Ma Y, Luo X, et al. 2017. The discovery of surface runoff in the megadunes of Badain Jaran Desert, China, and its significance. Science China Earth Sciences, 60: 707–719.

Zhu B Q. 2023. Paleo-atmospheric precipitation recharged to groundwater in middle-latitude deserts of Northern China. Atmosphere, 14: 774, doi: 10.3390/atmos14050774.